Gravitational Waves from Holographic Neutron Star Mergers

Christian Ecker

Universiteit Utrecht

Cern – 8 October 2019

Based on arXiv:1908.03213

with Matti Järvinen, Govert Nijs and Wilke van der Schee

Neutron star merger with holographic EoS

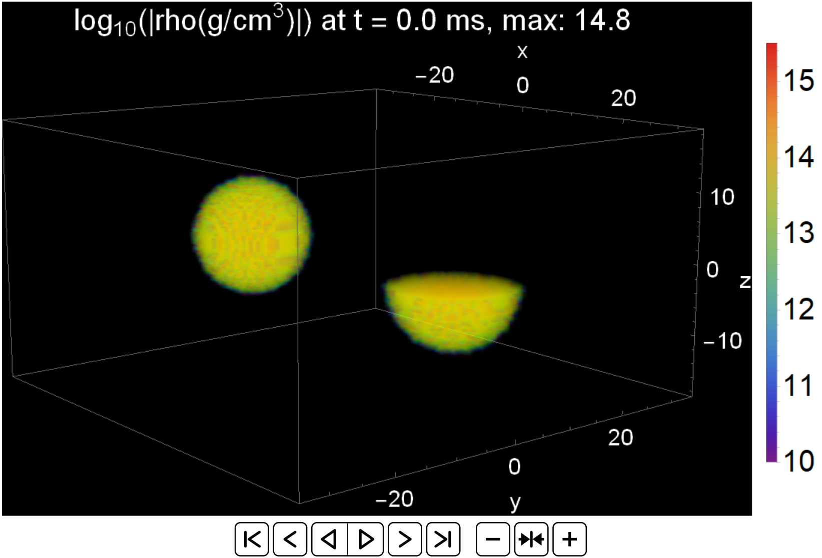

Outline

1. Introduction

Neutron stars

- Neutron stars (NSs) are born in supernova explosions of massive ($8 - 25 M_\odot$) main sequence stars.

- Densest astrophysical objects which are not black holes (BHs)

$$M \approx 1.4 M_\odot, \quad R \approx 10\mathrm{km}, \quad \rho \approx 2 - 5\rho_0$$

  (nuclear saturation mass-energy density $\rho_0 = 2.5 \cdot 10^{14} \mathrm{g\,cm}^{-3}$)

- Can have huge magnetic fields (magnetars) $B \approx 10^{15}\mathrm{G}$
  (cf. earth: $B_\oplus \approx 0.6\mathrm{G}$, RHIC: $B_{HIC} \approx 10^{18}\mathrm{G}$)

- Some rotate extremely fast (pulsars) $\nu_{\mathrm{rot}} \lessapprox 1\mathrm{ms}^{-1}$
  first detection in 1967 as pulsar = rapidly rotating and highly magnetized NS
  record holder: PSR J1748-2446ad ($v_R \approx 0.24c$)

- Neutron stars are cool: T in keV range
  $T \ll \Lambda_{QCD} \implies T = 0$ good approx., located at bottom of QCD phase diagram.
  neutrino cooling: from $10^{11}K \approx 10\mathrm{MeV}$ after supernova to keV within days.
  shock heating: finite temperature contributions become important during merger.

Neutron star binaries

- Binary NS systems are most likely formed in main-sequence star binaries[1], less likely by dynamical capture.
- First discovery in 1974: Hulse-Taylor binary pulsar (PSR B1913+16), successful test of Einstein gravity and indirect proof for gravitational waves (GWs).
- Known binary NS systems typically have: [J.M. Lattimer 2012, see also www.stellarcollapse.org]
    - Masses around $M_{1,2} \approx 1.4 M_\odot$
    - Mass ratio $q \equiv M_1/M_2 \approx 1$
    - Several million years of inspiral phase, i.e. enough time to cool down by neutrino cooling and circularize orbits by GW emission.

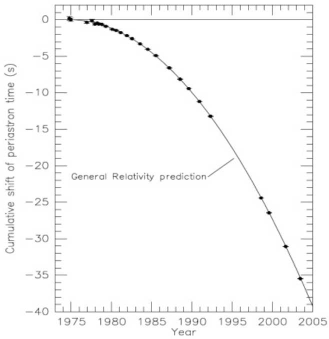

[picture: Weisberg, Taylor astro-ph/0407149]

[1] Most stars (up to $\approx 85\%$) are actually in binary systems. (see www.atnf.csiro.au)

Neutron star mergers

- Significant sources of gravitational radiation.
- Microscopic properties of dense matter encoded in GW and EM signal.
- Likely the origin of short gamma-ray bursts (SGRBs)
- and of heavy elements like gold, platinum, or uranium.

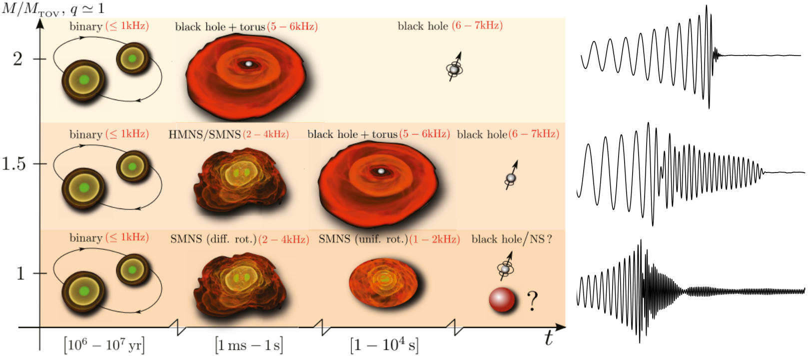

[picture: Baiotti, Rezzola arXiv:1607.03540]
(SMNS: $M_{\rm TOV} < M < M_{\rm max} \approx 1.2 M_{\rm TOV}$, HMNS: $M > M_{\rm max}$)

Neutron star equation of state

- Equation of state (EoS) $p(\epsilon, T, \ldots)$ required to close EOMs in fluid description of neutron stars.
- EoS determines[2] mass-radius relation of isolated star.
- First principle QCD calculations at relevant μ not feasible:
  - pQCD only at asymptoticaly large μ and/or T.
  - Lattice QCD has sign problem at finite μ.
- Nuclear matter models typically only reliable for $\rho \lessapprox \rho_0$.

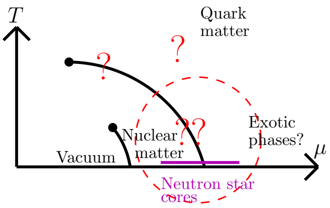

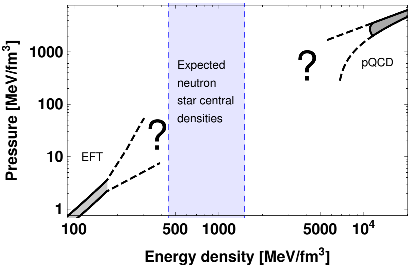

[2] For a given EoS the mass-radius relation is obtained by solving the Tolman-Oppenheimer-Volkov (TOV) equations.

Observational constraints

- Mass measurement of NS-white dwarf binary PSR J0348+0432 provides lower bound on maximal mass: $M_{\mathrm{max}} > 2.01 \pm 0.04 M_{\odot}$.
  [Antoniadis et. al. arXiv:1304.6875]
- LIGO/Virgo detection GW170817: only inspiral phase was accessible, enough to constrain tidal deformability[3], EoS can not be too stiff: $\Lambda \lessapprox 600$.
  [LIGO/Virgo: arXiv:1710.05832, arXiv:1805.11579, arXiv:1805.11581]

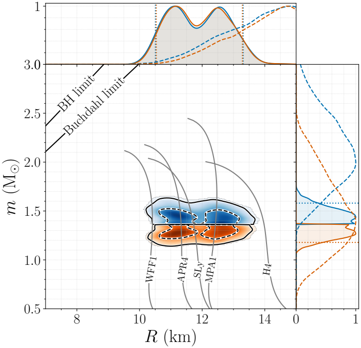

[3]Tidal deformability: $\Lambda = \frac{2}{3} k_2 \left(c^2 R/(Gm)\right)^5$, mass m, radius R, Love number k_2

2. Holographic Model

Holographic model: V-QCD

Bottom-up construction with dynamical quark and gluon sectors and potentials tuned to mimic QCD.

Two building blocks of Veneziano QCD (V-QCD):

1. Improved holographic QCD (IHQCD) for gluon sector (dilaton gravity).
   [Gürsoy, Kiritsis, Nitti; Gubser, Nellore]
2. Sen-like tachyonic Dirac-Born-Infeld (DBI) actions for flavor sector and chiral symmetry breaking via tachyon condensation.
   [Bergman, Seki, Sonnenschein; Dhar, Nag; Bigazzi, Casero, Cotrone, Kiritsis, Paredes; Gürsoy, Kiritsis, Nitti; Iatrakis, Kiritsis, Paredes]

Consider 1. + 2. in the Veneziano limit with full backreaction:

$$N_c \to \infty \text{ and } N_f \to \infty \text{ with } x \equiv N_f/N_c \text{ fixed}$$

[Järvinen, Kiritsis arXiv:1112.1261]

Add probe baryons: simple approximation with homogeneous bulk soliton. One free parameter: b = coupling between baryon and chiral condensate.

[Ishii, Järvinen, Nijs arXiv:1903.06169]

Phase diagram

- Baryons appear at medium μ in the confined phase
- Nontrivial nuclear and quark matter EoS from the same model
- Free parameter of the holographic model b chosen to set the correct μ_c at vacuum-baryon transition

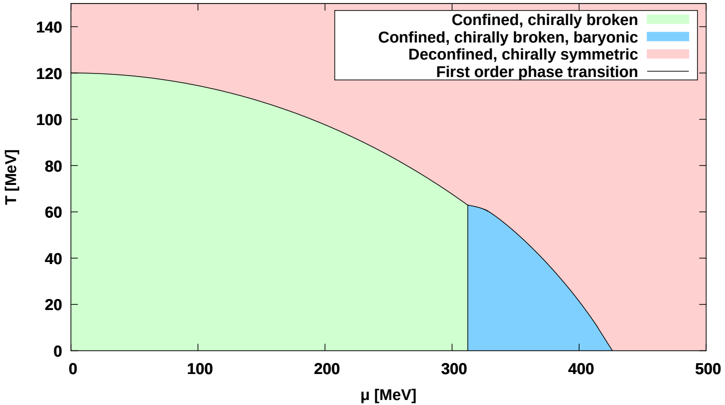

[Ishii, Järvinen, Nijs arXiv:1903.06169]

Hybrid Equation of State (I)

Construction of the hybrid EoS:

- In the crust and for low densities (up to $1.5 - 2\rho_0$) we use the SLy nuclear matter EoS. Here the nuclear matter EoS is expected to be more reliable than the holographic model.
[Haensel, Pichon nucl-th/9310003, Douchin, Haensel astro-ph/0111092]
- For dense nuclear matter the baryonic V-QCD is matched[4] to SLy.
- Baryon onset in SLy part $\Longrightarrow$ freedom in holographic parameter b.
- Changing b shifts μ_{match} $\Longrightarrow$ more/less SLy at low densities.
- At high densities the V-QCD EoS transitions to the quark phase $\Longrightarrow$ same model for holographic baryon and quark phase.

[4] Matching point μ_{match} and normalization c_b of the action are chosen to give continuous $p(\mu)$ and $p'(\mu)$ at matching point.

Hybrid Equation of State (II)

- Second order phase transition at matching between SLy and VQCD.
- Strong[5] first order nuclear to quark matter phase transition.
- LIGO observation GW170817 constrains $b \gtrapprox 10.45 \rightarrow \Lambda_{1.4} \approx 680$.

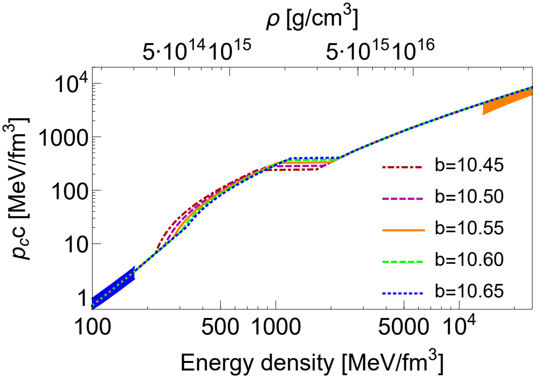

b	$\frac{\rho_m}{\rho_s}$	$\Lambda_{1.4}$
10.45	1.44	680
10.50	1.61	550
10.55	1.77	470
10.60	1.94	410
10.65	2.10	370
SLy	–	300

[5] The latent heat at the transition is sizable (for $b = 10.5$: $\Delta\epsilon = 920\mathrm{MeV/fm^3}$).

Mass-radius relation

- Large values of $b \gtrsim 10.65$ are ruled out by $2.01M_\odot$-bound from PSR J0348+0432 and PSR J1614-2230.

  [Demorest et. al. arXiv:1010.5788, Antoniadis et. al. arXiv:1304.6875]

- Allowed values in the holographic model: $10.45 \lesssim b \lesssim 10.65$.

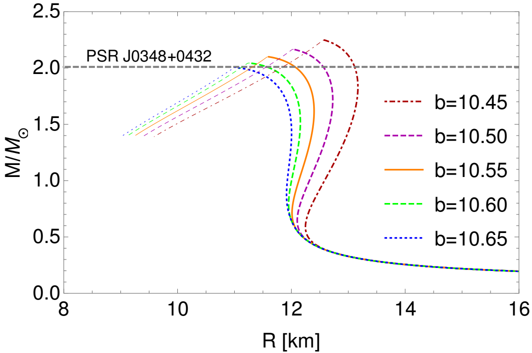

b	$\frac{R_{1.4}}{km}$	$\frac{M_{\max}}{M_\odot}$
10.45	13.0	2.25
10.50	12.6	2.17
10.55	12.3	2.10
10.60	12.1	2.04
10.65	12.0	2.00
SLy	11.7	2.05

Hybrid Equation of State (III)

The resulting EoS for $b = 10.5$ compares nicely with the generic analysis of reasonable polytropic interpolations.

[Annala, Gorda, Kurkela, Nättila, Vuorinen arXiv:1903.09121]

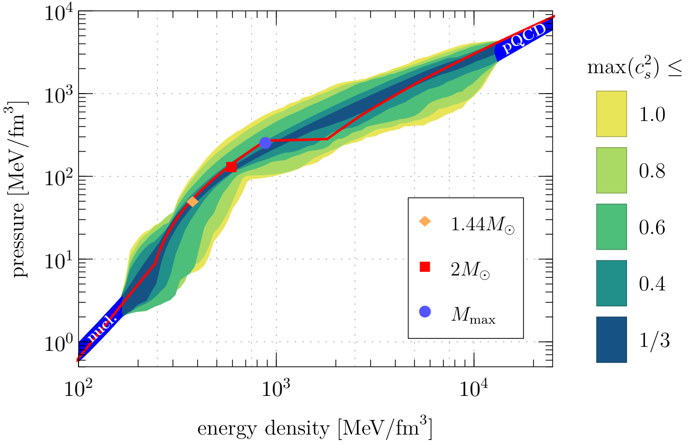

[plot by T. Gorda]

3. Merger Simulations

Simulating neutron star mergers (I)

Have to evolve the 4D general relativistic hydrodynamics equations:

$$R_{\mu\nu} - \frac{1}{2} R g_{\mu\nu} = 8\pi G_N T_{\mu\nu}\,, \quad \nabla_\mu T^{\mu\nu} = 0\,, \quad \nabla_\mu J^\mu = 0\,, \quad p = p(\epsilon),$$

$$ds^2 = -(\alpha^2 - \beta^i \beta_i) dt^2 + 2\beta_i dx^i dt + \gamma_{ij} dx^i dx^j\,,$$

with initial conditions (spacetime and fluid distribution) modelling a NS binary system:

- Use pseudo spectral code `LORENE`[6] to generate initial data.

  [Gourgoulhon, Grandclement, Taniguchi, Marck, Bonazzola arXiv:gr-qc/0007028]

- Assumes helical symmetry = circularity of the BNS orbit, no GWs.
- Use non-spinning ICs for the fluid distribution.
- Initial distance D must be sufficiently large to justify circular orbit approximation, but not too large (reasonable inspiral time).
  Use $D = 45\mathrm{km}$, gives between three ($1.4 M_\odot$) and six ($1.3 M_\odot$) orbits.

[6] Langage Objet pour la RElativite NumeriquE, see http://www//lorene.obspm.fr

Simulating neutron star mergers (II)

Einstein equations need to be solved in strongly hyperbolic[7] form.

- Use Conformal and Covariant Z4 (CCZ4) formulation
  [Alic, Bona-Casas, Bona, Rezzolla, Palenzuela]
- Lapse α and shift β^i fixed by singularity avoiding gauge conditions.
- Implemented in the `Einstein Toolkit`.
  [Löfler et. al., arXiv:1111.3344, http://einsteintoolkit.org]
- Hydro equations solved with `WhiskyTHC`[8].
  [Radice, Rezzolla arXiv:1206.6502]

[7] The weakly hyperbolic ADM formulation (metric γ_{ij} and the extrinsic curvature K_{ij} as dynamical variables) does not lead to stable time evolution.

[8] see D. Radices homepage: https://www.astro.princeton.edu/ dradice/index.html

Spacetime discretization

- Grid must be large enough to extract GW in "asymptotic" region.
- Fine enough to resolve the NS, merger dynamics and BH formation.
  $\Longrightarrow$ Adaptive mesh refinement (AMR) required.
- We use a cubic grid of $\approx 3025\mathrm{km}$ ($\approx 70D$) side length.
- Reflection symmetry about xy-plane.
- Six "refinement levels":
  Coarse mesh ($\Delta h_0 \approx 23.5\mathrm{km}$) in the asymptotic region.
  Finest meshes ($\Delta h_6 \approx 365\mathrm{m}$) centered at the neutron stars.
  $\Longrightarrow \approx 5 \cdot 10^6$ gridpoints and $\approx 5 \cdot 10^5$ time steps!

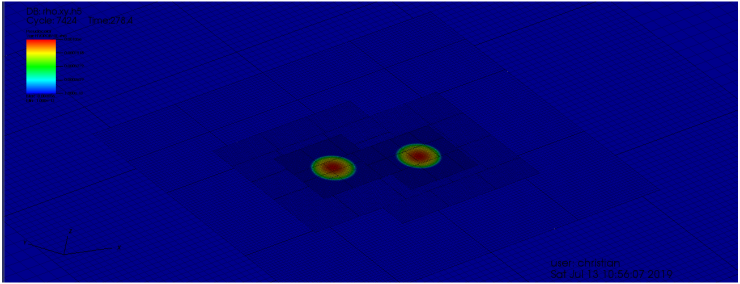

Supercomputing

- To simulate neutron stars one needs supercomputing.
- Pilot project (500.000 CPUh) on Dutch supercomputer Cartesius.
  [https://userinfo.surfsara.nl/systems/cartesius]
- Typical simulation costs 10.000 CPUh on 100 CPUs and takes $\approx$ 4 days.

Extracting Waveforms

- Extract Newman-Penrose scalar ψ_4 from simulation

$$\psi_4 := C_{\mu\nu\rho\sigma} k^\mu \bar{m}^\nu k^\rho \bar{m}^\sigma \,, \quad \text{null tetrade: } \{l^\mu, k^\mu, m^\mu, \bar{m}^\mu\} \,.$$

- The GW polarization amplitudes (h_+,$h_\times$) are related to ψ_4 via [see e.g. book by M. Alcubierre (2005)]

$$\ddot{h}_+ - i\ddot{h}_\times = \psi_4 = \sum_{\ell=2}^{\infty} \sum_{m=-\ell}^{\ell} \psi_4^{\ell m} \, {}_{-2}Y_{\ell m}(\theta, \varphi) \,.$$

- Consider only the dominant $\ell = m = 2$ mode

$$h_{+,\times} = \sum_{\ell=2}^{\infty} \sum_{m=-\ell}^{\ell} h_{+,\times}^{\ell m} \, {}_{-2}Y_{\ell m}(\theta, \varphi) \approx h_{+,\times}^{22} \, {}_{-2}Y_{22}(\theta, \varphi) \,,$$

  and assume optimal orientation (${}_{-2}Y_{22}(0,0) = \frac{1}{2}\sqrt{5/\pi}$) of the merger with respect to the detector.
- Extrapolate signal to detector, assume distance of $40\mathrm{Mpc}$, i.e. same luminosity distance as GW170817.

Power Spectral Density

Post-merger power spectral density (PSD) has typical three peak structure.

$$\tilde{h}(f) \equiv \sqrt{\frac{|\tilde{h}_+(f)|^2 + |\tilde{h}_\times(f)|^2}{2}}\,, \quad \tilde{h}_{+,\times}(f) \equiv \int h_{+,\times}(t) e^{-i2\pi f t} dt\,.$$

Characteristic frequencies f_1, f_2, f_3 contain information about EoS.
[Takami, Rezzolla, Baiotti arXiv:1403.5672]

Strategy: simulate predictions for f_1, f_2, f_3 and compare to future observations.

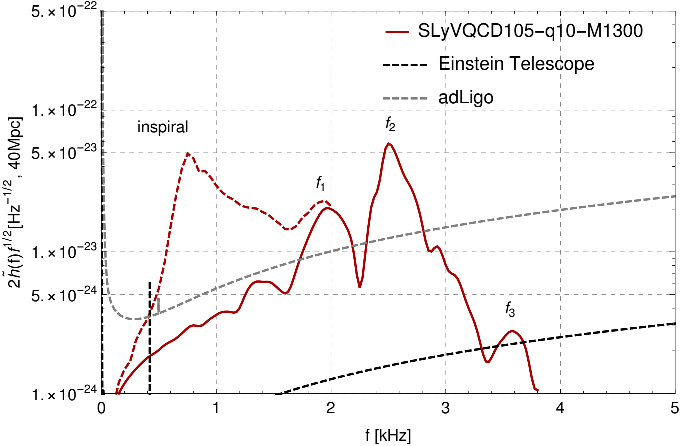

4. Results

High mass binary

- Equal mass binary $M_1 = M_2 = 1.5M_\odot$ with $b = 10.5$ SLy+VQCD EoS.
- Prompt collapse to BH with dilute matter torus $\rightarrow$ tivial post-merger PSD.
- Densities are not high enough to create quark matter outside BH.

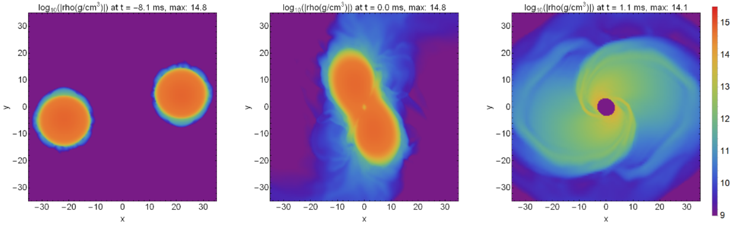

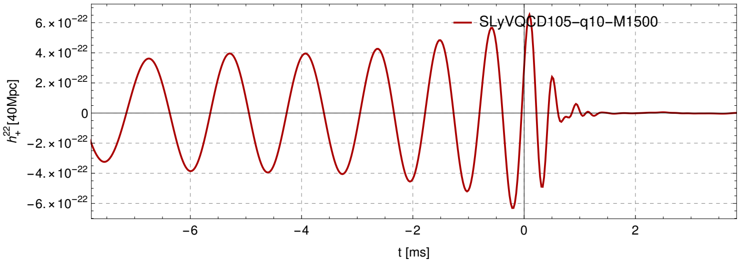

Intermediate mass binary

- Equal mass binary $M_1 = M_2 = 1.4M_\odot$ with $b = 10.5$ SLy+VQCD EoS.
- Formation of a short lived ($\approx 7.8ms$) HMNS $\rightarrow$ non-trivial PSD.

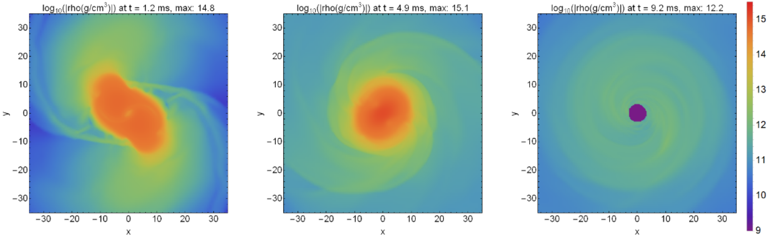

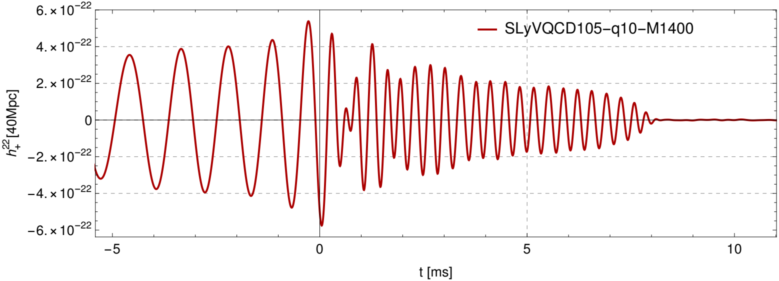

Low mass binary

- Equal mass binary $M_1 = M_2 = 1.3 M_\odot$ with $b = 10.5$ SLy+VQCD EoS.
- Formation of a long lived ($> 40 ms$) HMNS $\rightarrow$ non-trivial PSD.

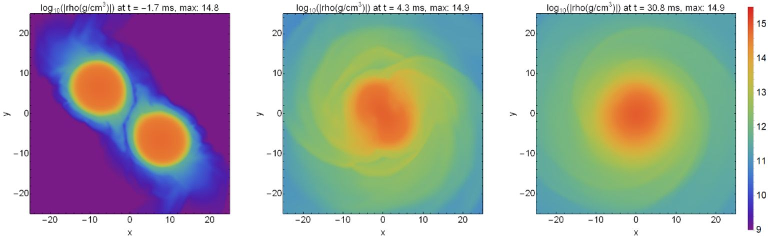

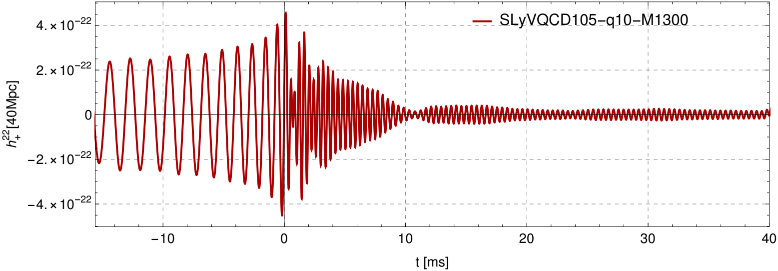

Mass dependence of the Power Spectral Density

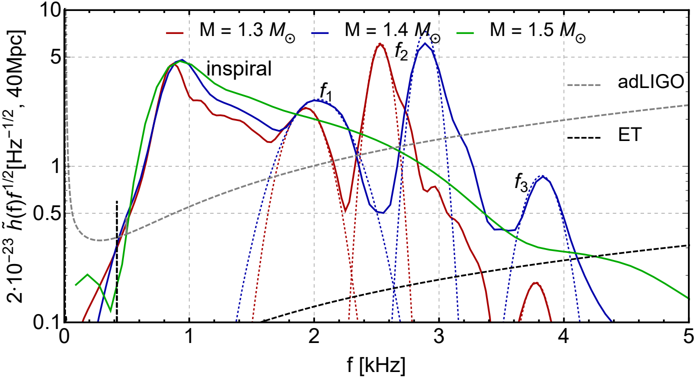

$M[M_\odot]$	EoS	b	f_1 [kHz]	f_2 [kHz]	f_3 [kHz]
1.30	SLyVQCD105	10.5	1.93	2.53	3.77
1.35	SLyVQCD105	10.5	1.95	2.60	3.53 (3.90)
1.40	SLyVQCD105	10.5	2.03	2.89	3.82
1.50	SLyVQCD105	10.5	–	–	–

EoS dependence of the Power Spectral Density

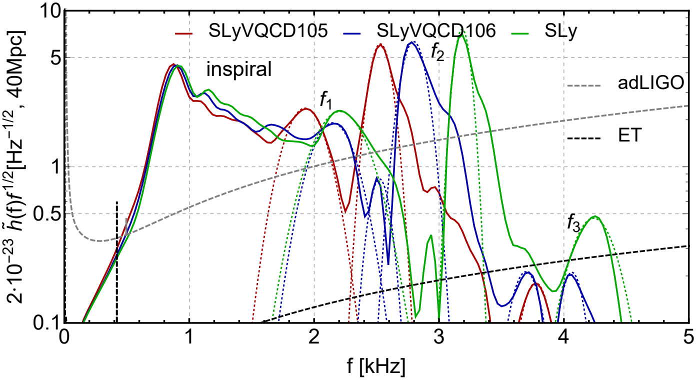

$M[M_\odot]$	EoS	b	f_1 [kHz]	f_2 [kHz]	f_3 [kHz]
1.30	SLyVQCD105	10.5	1.93	2.53	3.77
1.30	SLyVQCD106	10.6	2.15	2.80	3.70 (4.06)
1.30	SLy	-	2.21	3.19	4.24

Universality

- Frequency f_1 as function of compactness $\mathcal{C} = M/R$ shows universal behaviour, i.e. results for different EoS fall on one universal curve.
- V-QCD EoS for $b = 10.5$ gives f_1 close to universal curve, $b = 10.6$ slightly off (?) $\Longrightarrow$ more analysis needed.

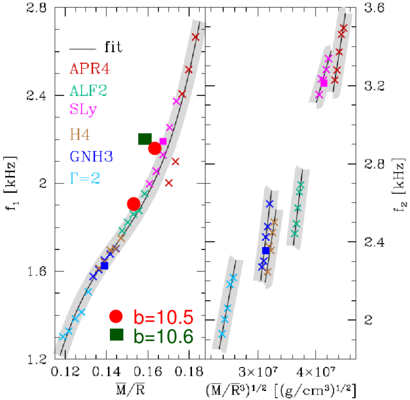

[plot from Takami, Rezzolla, Baiotti arXiv:1403.5672]

5. Summary and Outlook

Summary

- Constructed "realistic" hybrid holographic EoS that satisfies all currently known theoretical and observational constraints.
- First NS merger simulations using input from holography.
- Predictions for characteristic peaks in power spectral densities
  $\Longrightarrow$ new connection between holography and experiment!
- Preliminary results show slight violation of universality for f_1, more accurate simulations necessary to draw conclusions.

Outlook

- Increase resolution to improve accuracy of waveforms and PSD (costly!).
- Include finite T effects in EoS $\rightarrow$ temperature driven de-confinement phase transition.
- Spin, non-equal mass binaries, NS-BH merger, magnetic fields.
- Improve holographic model:
  - go beyond homogeneous baryon ansatz: numerical solutions for inhomogeneous solitons.
  - include magnetic field dependence in the EoS.
  - systematic study with different nuclear matter EoSs at low density.
- Only first step towards holographic GW model building, lots of possibilities and challenges!

6. Backup

V-QCD without baryons (I)

Consider first the non-baryonic V-QCD action, whose solutions will serve as background for the probe baryons

$$S^{(0)}_{\mathrm{V-QCD}} = S_{\mathrm{glue}} + S^{(0)}_{\mathrm{DBI}} .$$

The gluon part is given by the IHQCD (dilaton gravity) action

$$S_{\mathrm{glue}} = N_c^2 M^3 \int d^5x \sqrt{-g} \left[R - \frac{4}{3}\frac{(\partial\lambda)^2}{\lambda^2} + V_g(\lambda) \right] ,$$

where $\lambda \equiv e^{\phi} \leftrightarrow \mathrm{Tr} F^2$ ($\approx g^2 N_c$ near the boundary) sources the 't Hooft coupling in YM theory, the dilaton potential is chosen[9] to mimic QCD

$$V_g(\lambda) = 12 \left[1 + V_1 \lambda + \frac{V_2 \lambda^2}{1+\lambda/\lambda_0} + V_{\mathrm{IR}} e^{-\lambda_0/\lambda} (\lambda/\lambda_0)^{4/3} \sqrt{\log(1+\lambda/\lambda_0)} \right] .$$

Finite T is implemented by homogeneous+isotropic black brane metric

$$ds^2 = e^{2A(r)}(-f(r)dt^2 + d\vec{x}^2 + f^{-1}(r)dr^2) .$$

[9] E.g. V_1 and V_2 are fixed by requiring the UV RG flow of the 't Hooft coupling to be the same as in QCD up to two-loop order.

V-QCD without baryons (II)

The flavor part is modelled by the tachyonic DBI-action[10]

$$S_{\mathrm{DBI}}^{(0)} = -N_f N_c M^3 \int d^5x\, V_{f0}(\lambda) e^{-\tau^2} \sqrt{-\det\left[g_{ab} + \kappa(\lambda)\partial_a\tau\partial_b\tau + w(\lambda)F_{ab}\right]}\,,$$

$$F_{rt} = \Phi'(r)\,, \quad \Phi(0) = \mu\,,$$

where the tachyon $\tau \leftrightarrow \bar{q}q$ controls chiral symmetry breaking.

Several potentials: $\{V_g(\lambda), V_{f0}(\lambda), w(\lambda), \kappa(\lambda)\}$, chosen to match pQCD in UV ($\lambda \to 0$), qualitative agreement with QCD in IR ($\lambda \to \infty$) and tuned to lattice QCD in the middle ($\lambda \sim \mathcal{O}(1)$).

[For details see Appendix B of Ishii, Järvinen, Nijs arXiv:1903.06169]

Different solutions:

without/with horizon $\leftrightarrow$ confined/deconfined phase
without/with tachyon $\leftrightarrow$ chirally symmetric/chirally broken phase

[10] Without baryons we have a vectorial flavor singlet gauge field $A^{(L/R)} = \mathbb{I}_f \Phi(r) dt$ giving nonzero charge density and chemical potential.

Probe baryons in V-QCD

Each baryon maps to a solitonic "instanton" configuration of non-Abelian gauge fields in the bulk.

[Witten; Gross, Ooguri; ...]

Consider the full non-Abelian brane action $S = S_{\rm DBI} + S_{\rm CS}$ where

[Bigazzi, Casero, Cotrone, Kiritsis, Paredes; Casero, Kiritsis, Paredes]

$$S_{\rm DBI} = -\frac{1}{2} M^3 N_c \, \mathbb{T}r \int d^5x \, V_{f0}(\lambda) e^{-\tau^2} \left(\sqrt{-\det \mathbf{A}^{(L)}} + \sqrt{-\det \mathbf{A}^{(R)}} \right) ,$$

$$\mathbf{A}^{(L/R)}_{MN} = g_{MN} + \delta^r_M \delta^r_N \kappa(\lambda) \tau'(r)^2 + \delta^{rt}_{MN} w(\lambda) \Phi'(r) + w(\lambda) F^{(L/R)}_{MN}$$

gives the dynamics of the solitons.
The Cern-Simons term sources the baryon number for the solitions

$$S_{\rm CS} = \frac{N_c}{8\pi^2} \int \Phi(r) e^{-b\tau^2} dt \wedge \left(F^{(L)} \wedge F^{(L)} - F^{(R)} \wedge F^{(R)} + \cdots \right) .$$

Non-Abelian DBI action only known to first few orders in $F^{(L/R)}$: expand to second order on top of solution $(g_{MN}, \Phi, \lambda, \tau)$ obtained from $S^{(0)}_{V-QCD}$.

Homogeneous Baryon Ansatz

Set $N_f = 2$ and consider the SU(2) Ansatz

[Rozali, Shieh, Van Raamsdonk, Wu]

$$A_L^i = -A_R^i = h(r)\sigma^i$$

Immediate consequence: baryon charge integrates to zero?

$$N_b \propto \int dr \frac{d}{dr}\left[e^{-b\tau^2} h^3(1 - 2b\tau^2)\right] \stackrel{?}{=} 0$$

However finite baryon number may can be realized by discontinuity of h $\leftrightarrow$ smeared solitons in singular gauge.

[Ishii, Järvinen, Nijs, arXiv:1903.06169]

The free parameter b of the model is used to tune the baryon onset to its physical value in QCD.